



Optimizing Sulfuric Acid 98% Leaching: Lithium Recovery from Madagascar Spodumene

Rabearisoa Solotiana Rija^{1,2} Robijaona Rahelivololoniaina Baholy^{1,2}

¹Industrial, Agricultural and Food Process and Systems Engineering, Doctoral School, University of Antananarivo, Antananarivo, Madagascar

²Polytechnic School of Antananarivo, University of Antananarivo, Antananarivo, Madagascar
Email: robijob111@gmail.com

Abstract: A comprehensive study of lithium extraction from Vakinankaratra, Madagascar spodumene through sulfuric acid digestion and subsequent aqueous leaching is presented. The process initiates with calcination, a pretreatment designed to induce the alpha-to-beta phase transformation of spodumene, resulting in decreased density, increased friability, and enhanced chemical reactivity. Characterization of the ore, employing X-ray fluorescence (XRF) and atomic absorption spectroscopy (AAS), revealed a mineralogical composition dominated by oxides of lithium, silicon, aluminum, potassium, and fluorine, confirming the presence of economically relevant lithium concentrations. The investigation explored the influence of reaction time, varying from one to three hours, at elevated digestion temperatures. Rigorous optimization of experimental parameters was conducted, yielding significant insights into the leaching process. The findings demonstrate a strong correlation between lithium extraction efficiency and the ore-to-acid ratio, temperature, and, most notably, reaction time. Under optimized conditions, specifically a reaction temperature of 250°C and a duration of three hours, a 92% lithium extraction rate was achieved for both calcined spodumene and lepidolite samples. This study provides a detailed understanding of the critical parameters governing lithium extraction from Malagasy spodumene, contributing to the development of efficient and industrially applicable extraction methodologies.

Keywords: Lithium, spodumene, extraction, calcination, sulfuric acid

I. Introduction

Lithium assumes a pivotal role within contemporary technological paradigms, notably in the fabrication of rechargeable batteries for electronic devices, electric vehicles, and energy storage systems. Its strategic importance is further amplified by the global transition towards clean and renewable energy sources. The International Energy Agency's (IEA) "Global EV Outlook 2021" report projects a substantial increase in lithium-ion battery demand in the forthcoming years, driven by the expanding electric vehicle market. This surge is attributed to lithium's unique electrochemical properties, characterized by the highest electrochemical potential among alkali metals coupled with its exceptionally low atomic mass. (Swain, 2017 ; Deberitz, 2003 ; Schmidt, 2017)

Presently, approximately 80% of global lithium demand is attributed to battery manufacturing, while traditional applications, including ceramics and glass (7%), industrial lubricants (4%), continuous casting agents (2%), air treatment (1%), and pharmaceuticals (1%), constitute a comparatively minor portion of its utilization (U.S. Geological Survey, 2023).

While lithium exhibits relative geological abundance, its economically viable extraction is confined to specific geological formations, primarily continental brines and granitic

pegmatites. Pegmatites, despite their lithium richness, are generally characterized by smaller deposit sizes and lower estimated total resources compared to alternative mineable sources (Holleman *et al.*, 2016; Meshram *et al.*, 2014 ; Garrett, 2004).

Lithium-bearing pegmatites, such as those containing spodumene and lepidolite, represent significant lithium sources, with lithium concentrations ranging from 1.37% to 3.6% Li (Dinh, 2015). The abundance and lithium content of these minerals establish them as critical resources for lithium extraction. Spodumene, a lithium silicate, stands as one of the principal commercial sources of lithium.

The imperative for technological advancements in lithium mineral beneficiation, encompassing physical concentration and metallurgical processing, is evident to facilitate the competitive production of lithium-based compounds in salt, hydroxide, and carbonate forms (Margarido *et al.*, 2014). Over extended periods, methodologies for lithium recovery from pegmatitic rock have been developed and, in certain instances, implemented on a relatively limited scale (Sahoo *et al.*, 2024 ; Tadesse *et al.*, 2019)

Lithium mineral processing typically involves the chemical roasting of concentrates utilizing acidic reagents (hydrochloric, sulfuric, or hydrofluoric acid), basic reagents (lime, sodium hydroxide, or limestone), and salts (sodium or potassium salts) (Nandihalli *et al.*, 2024 ; Fosu *et al.*, 2020). Given the inherent resistance of lithium-based silicates to chemical attack, metallurgical processes invariably incorporate an initial calcination stage, conducted at temperatures ranging from 750 to 1100°C, to enhance reactivity. This is subsequently followed by hydrometallurgical stages, employing acid digestion and leaching, to generate soluble lithium compounds (Nogueira *et al.*, 2014).

Digestion of lithium minerals with sulfuric acid gives high lithium yields and favorable energy consumption compared with other processes. (Marcinov *et al.*, 2023 ; Kondas & Jandová, 2006 ; Habashi, 1997). Sulfuric acid is also easier to handle than other acids. (Sitando & Crouse, 2011)

The escalating demand for lithium within the contemporary global market, driven by its application in electric and hybrid vehicle batteries, energy storage devices, and established lithium industry processes, necessitates a focused research initiative. A project entitled 'Lithium Extraction from Spodumene and Lepidolite Pegmatites in the Sahatany Valley, Antsirabe II District, Madagascar, Utilizing Sulfuric Acid Digestion' has been undertaken to address this imperative.

This investigation seeks to elucidate optimal extraction methodologies for lithium from Malagasy pegmatite resources, thereby contributing to the development of sustainable and efficient lithium recovery processes. The study will encompass a comprehensive analysis of the physicochemical parameters influencing sulfuric acid digestion, with a focus on maximizing lithium yield and minimizing environmental impact.

II. Research Methods

2.1 Présentation of the study area

Madagascar possesses notable mining potential for strategic minerals, including spodumene and lepidolite, both significant sources of lithium essential for battery production. These minerals occur across multiple Malagasy sites, manifesting as pegmatitic veins or disseminated within specific magmatic rock formations.

The Sahatany Antsirabe II deposit, the focal point of this investigation, is situated within the Sahatany Valley, located in the Vakinankaratra region of central Madagascar, approximately 25 kilometers southwest of Antsirabe. This region is characterized by its

temperate climate and abundant mineral resources. The Sahatany Valley is geologically diverse, hosting numerous lithium-bearing pegmatites (**Ranoroso, 1986**).

The deposit encompasses an area of approximately 150 square kilometers and exhibits a high degree of mineralogical complexity, including spodumene, lepidolite, and various tourmaline species. The deposit's strategic geographical location, coupled with its substantial mineral endowment, establishes it as a critical site for lithium extraction, a resource of increasing industrial significance. (**Mindat, 2024 ; Raheisoa, 2017 ; Rakotoarisoa, 2003 ; Rakotovao, 2004**). Tsy misy an'io Mindat io ao amin'ny liste des références biblio nataonao, ampio an'io raha itanao fa aleo esorina raha tsy ita



Figure 1. Overview of the Antokambohitra, Tsarafara and northwestern Sahatany valley primary and eluvial lithiferous pegmatite deposits. (**Source: Rabearisoa, année**) Azafady, ataovy en anglais ireo soratra ireo

A comprehensive mineralogical and geochemical characterization of the Antokambohitra and Tsarafara primary and eluvial lithium-bearing pegmatite deposits, located northwest of the Sahatany Valley, is presented. This overview encompasses a detailed assessment of the deposit's geological context, mineralogical composition, and the distribution of lithium-bearing phases within both primary and eluvial formations. The analysis aims to elucidate the potential for economically viable lithium extraction from these deposits, providing critical data for resource evaluation and process development.

2.2 Raw materials

The ore samples utilized in this study were sourced from the Sahatany manual drilling mine site, specifically from locations defined by the following geographical coordinates: S 019° 42' 19" E 046° 54' 25" (Tsarafara, figure 2a) and S 020° 03' 12" E 046° 57' 22" (Antokambohitra, figure 2b).



Figure 2a. Quarry at the Tsarafara primary pegmatite deposit (Source: Rabearisoa, année)




Figure 2b : Antokambohitra eluvial spodumene and lepidolite deposits (Source: Rabearisoa, année)

These coordinates delineate the precise locations from which the ore samples were extracted, providing a spatially referenced context for the subsequent mineralogical and chemical analyses. The utilization of manually extracted ore from these specific locations permits a focused investigation into the local mineralogical variations and lithium-bearing phase distribution within the Sahatany region.

Four distinct samples, each weighing 3 kilograms, were collected from each designated site, indexed according to their respective geographical coordinates. The following table provides a comprehensive listing of the ore samples obtained from the aforementioned location zones.

Table 1. Geographical coordinates of the 4 samples

Code Samples	Geographical location	Photos of samples	Location
SPOD A1	S 020° 05' 24" E 046° 56' 02"		Antokambohitra




SPOD A2	S 020° 03' 12" E 046° 57' 22"		Antokambohitra
SPOD T1	S 019° 59' 05" E 046° 57' 08"		Tsarafara
SPOD T2	S 019° 42' 19" E 046° 54' 25"		Tsarafara

Table 1 provides a concise tabulation of the geographical coordinates associated with each of the four collected samples, facilitating precise spatial referencing and enabling a detailed comparative analysis of the mineralogical and chemical compositions across the sampled locations.

2.3 Method

The qualitative and quantitative attributes of the collected samples were ascertained through a series of analytical procedures. Mineralogical analysis was conducted to determine the constituent mineral species within the ores, while chemical analysis provided a comprehensive elemental composition. Additionally, particle size distribution analysis was performed to elucidate the partitioning of recoverable elements across various size fractions.

This section further details the experimental methodology employed in the execution of the tests, outlining the procedural framework used to generate the analytical data. The presented methodology ensures reproducibility and allows for a rigorous assessment of the ore's characteristics.

a. Mineralogical analysis

A binocular vision microscope was employed to identify the major mineral species present within a sampled and pulverized ore specimen.

b. Chemical analysis

Elemental analysis of the sample was conducted using Energy Dispersive X-ray Fluorescence Spectrometry (EDXRF) on the S2 PUMA instrument and Flame Atomic Absorption Spectroscopy on the Perkin Elmer Optima instrument.

c. Particle size analysis

Subsequent to steaming, the spodumene sample was comminuted to a particle size of 500µm and utilized for particle size distribution analysis. This analysis was performed using a series of eight Tyler sieves, with mesh openings ranging from 63µm to 250µm, arranged on a Ro-Tap Model B sieve shaker.

2.4 Procedure

A finely ground sample underwent calcination in a laboratory electric furnace at temperatures ranging from 750°C to 1100°C for durations varying from 1.5 to 5 hours, with precise temperature control applied to the spodumene. This calcination process facilitates the transformation of α -spodumene to β -spodumene, a phase exhibiting enhanced reactivity towards acid attack, through thermally induced decrepitation. Subsequently, 100 grams of calcined β -spodumene and 100 grams of lepidolite, finely ground to 80µm, were weighed and placed in separate porcelain crucibles. Concentrated sulfuric acid (98%) was added to each crucible, maintaining defined ore-to-acid ratios (1:1, 1:2, 3:2, 3:4), and thoroughly mixed to form a homogeneous paste. Digestion was conducted at temperatures ranging from 175°C to

350°C (Meshram et al., 2014). The ore-acid mixtures were introduced into a laboratory furnace and maintained at the target temperature for durations spanning 0.5 to 3 hours. The resulting roasted materials were then cooled and dissolved in 250mL of water for one hour.

Following aqueous leaching at 90°C, excess sulfuric acid was neutralized with lime (Gmar & Chagnes, 2019), and the pH was adjusted to 7-10 to precipitate impurities such as iron and aluminum (GB/T51382, 2019), yielding a crude lithium sulfate solution with approximately 10% lithium oxide content (Tan et al., 2021 ; Kuang et al., 2018; Ran et al., 2016). Lime milk was subsequently introduced to remove residual magnesium and establish an alkaline environment (pH = 11-12) (GB/T51382, 2019; Ran et al., 2016; Zhu et al., 2008). Remaining calcium and magnesium ions were effectively removed through the addition of sodium carbonate (Su et al., 2019). The filtered solution was then evaporated and concentrated, resulting in a purified lithium sulfate solution with a lithium content exceeding 20%. Finally, lithium carbonate was precipitated by the addition of sodium carbonate, followed by centrifugation, dehydration, and drying to obtain the final lithium carbonate product. The relevant chemical equations are as follows:

1. $\text{Li}_2\text{O} \cdot \text{Al}_2\text{O}_3 \cdot 4\text{SiO}_2 + \text{H}_2\text{SO}_4 \rightarrow \text{Li}_2\text{SO}_4 + \text{Al}_2\text{O}_3 \cdot 4\text{SiO}_2 + \text{H}_2\text{O}$
2. $\text{Li}_2\text{SO}_4 + \text{Na}_2\text{CO}_3 \rightarrow \text{Li}_2\text{CO}_3 + \text{Na}_2\text{SO}_4$

III. Results and Discussion

3.1 Mineralogical analysis

A mineralogical identification of the major species present within a sampled and pulverized ore specimen was conducted utilizing binocular vision microscopy. The instrumentation employed for this analysis was a WILD HEERBRUGG microscope.

Table 2. Mineralogical composition of the samples studied

Mineral Species	Chemical Formula
Spodumene	$\text{LiAlSi}_2\text{O}_6$
Lepidolite	$\text{KLi}_2\text{Al}(\text{Al},\text{Si})_3\text{O}_{10}(\text{F},\text{OH})_2$
Alumina	Al_2O_3
Quartz	SiO_2
Muscovite	$\text{KAl}_2(\text{AlSi}_3\text{O}_{10})(\text{OH},\text{F})_2$

Microscopic observation revealed the presence of associated mineral constituents within the ore, namely quartz, muscovite, alumina, lepidolite, and spodumene. The corresponding observational data is presented in Table 2.

3.2 Chemical analysis

Elemental composition of the sample was determined through the application of Energy Dispersive X-ray Fluorescence Spectrometry (EDXRF) and Atomic Absorption Spectrometry (AAS). The resulting analytical data, detailing the presence and quantification of various elements, is presented in Table 3.

Table 3. Chemical composition of Spodumene studied

Elements	SPOD A1	SPOD A2	SPOD T1	SPOD T2
Al_2O_3	21.54	24.44	26.07	24.07
CaO	0.01	-	-	-
Cs_2O	0.02	0.01	0.05	0.05
Fe_2O_3	1.54	0.51	1.25	1.02

K₂O	4.78	3.27	2.07	1.87
Li₂O*	7.2	6.98	5.75	6.38
MgO	1.63	0.63	0.32	0.23
MnO	0.12	0.18	0.11	0.51
P₂O₅	0.19	0.49	0.15	0.09
SiO₂	66.43	59.90	54.90	58.90
TiO₂	0.03	0.01	0.01	0.01
Rb₂O	0.09	0.06	0.32	0.02
ZnO	0.02	0.04	0.01	0.01

A notable observation is the consistent presence of significant alumina (Al₂O₃) and silica (SiO₂) concentrations, indicative of the mineral's fundamental silicate structure. While the alumina content exhibits a moderate range, with SPOD T1 displaying the highest concentration, the silica content demonstrates a more pronounced variability, with SPOD A1 showing the highest value and SPOD T1 the lowest.

Lithium oxide (Li₂O), the element of primary interest, shows a relatively consistent presence across all samples, albeit with some variation. SPOD A1 and A2 possess higher Li₂O percentages, while SPOD T1 and T2 exhibit slightly lower values, yet still within a range deemed commercially significant.

Potassium oxide (K₂O) is present in appreciable quantities, particularly in SPOD A1, suggesting the presence of potassium-bearing minerals within the matrix. Iron oxide (Fe₂O₃) also appears in notable concentrations, indicating the potential for iron-related impurities. Magnesium oxide (MgO) and manganese oxide (MnO) are present in smaller, yet measurable quantities.

Trace elements such as cesium oxide (Cs₂O), rubidium oxide (Rb₂O), and zinc oxide (ZnO) are detected, albeit in minute concentrations. The presence of phosphorus pentoxide (P₂O₅) and titanium dioxide (TiO₂) is also noted, though their concentrations are generally low. Calcium oxide (CaO) is only present in SPOD A1, and absent in the other samples.

In essence, the data presented in Table 3 reveals a complex mineralogical composition, with significant variations in elemental concentrations across the sampled spodumene specimens. This variability necessitates a thorough understanding of the ore's specific characteristics to optimize lithium extraction processes.

3.3 Particle size analysis

A 1000-gram sample of dry ore, comminuted to a particle size of 250 µm, was subjected to particle size distribution analysis. This analysis was conducted using a series of six Tyler sieves, with mesh sizes ranging from 63 µm to 250 µm, arranged on a Ro-Tap model B sieve shaker.

Throughout the course of these analytical procedures, a balance was employed to ascertain the respective masses, expressed in grams, of the distinct particle size fractions.

Table 4 - Particle size analysis for spodumenes studied

Table 4 presents the particle size distribution of the spodumene samples, detailing the mass, cumulative weight, and cumulative percentage of particles within defined size fractions. This analysis provides a crucial understanding of the ore's physical characteristics, directly influencing subsequent processing and extraction efficiencies.

A notable observation is the distribution of mass across the various size fractions. For instance, the fraction ranging from -100 µm to +80 µm consistently exhibits the highest mass across all samples, indicating a significant concentration of particles within this range. Conversely, the fraction exceeding 250 µm demonstrates a minimal mass, suggesting a low proportion of larger particles.

The cumulative weight data illustrates the progressive accumulation of mass across decreasing particle sizes. Notably, the -63 μm fraction contributes significantly to the total cumulative weight, indicating a substantial presence of fine particles. This observation is further supported by the cumulative percentage data, which reveals that a significant proportion of the ore mass is concentrated within the finer size fractions.

Variations in particle size distribution are observed across the different spodumene samples. For example, SPOD T2 exhibits a higher concentration of particles within the -250 μm to +200 μm fraction compared to the other samples. These differences in particle size distribution may reflect variations in ore composition, geological origins, or processing history.

The data presented in Table 4 underscores the importance of particle size distribution analysis in characterizing spodumene ores. The observed variations in mass distribution and cumulative percentages provide valuable insights into the ore's physical properties, informing the design and optimization of extraction processes.

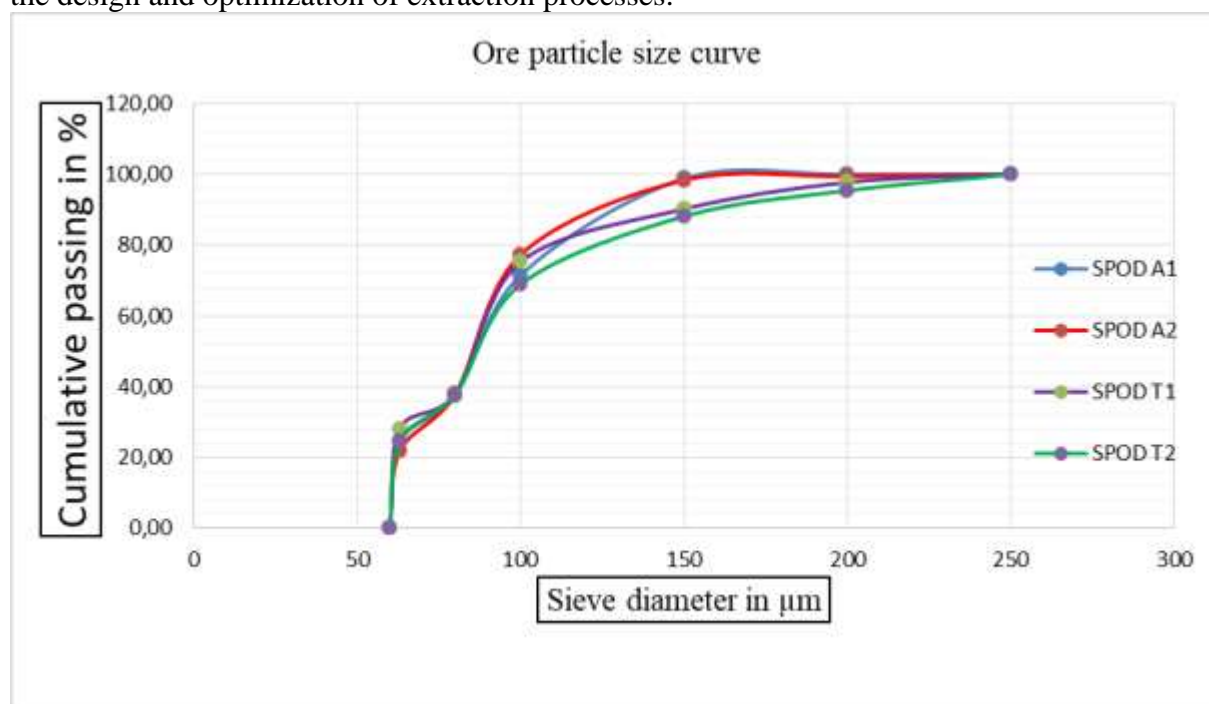


Figure 3. Graphical representation of ore particle size analysis

The data presented in Table 4 and Figure 3 reveals a significant concentration of the ore's mass within the particle size fraction ranging from 80 μm to 100 μm . Specifically, an average of 50.25% of the feed material is observed within this size range.

3.4 Digestion of α -spodumene with sulfuric acid

A series of preliminary tests was conducted to ascertain the necessity of high-temperature calcination of the ore. The results derived from these investigations are presented in Table 5.

Table 5 - Results of digestion tests on non-calcined α -spodumene ores

Essai	Ore/Acid ratio	Digestion temperature ($^{\circ}\text{C}$)	Time (h)	Li yield (%)			
				SPOD A1	SPOD A2	SPOD T1	SPOD T2
1	1:2	250	4	12.21	11.98	10.47	10.69
2	3:2	200	1	5.93	6.10	6.25	6.10

3	1 :1	300	2	8.37	9.24	10.01	9.89
4	3 :4	175	3	6.72	7.41	7.34	7.46

Table 5 presents the lithium yield obtained from a series of orientation tests, examining the influence of ore-to-acid ratio, digestion temperature, and reaction time on spodumene samples SPOD A1, SPOD A2, SPOD T1, and SPOD T2.

The data reveals a significant variation in lithium yield across the different experimental conditions. Notably, Test 1, conducted at an ore-to-acid ratio of 1:2, a digestion temperature of 250°C, and a reaction time of 4 hours, resulted in the highest lithium yields, ranging from 10.47% to 12.21% across the four samples. This observation suggests that a higher acid concentration and extended reaction time positively influence lithium extraction under these temperature conditions.

Conversely, Test 2, utilizing an ore-to-acid ratio of 3:2, a digestion temperature of 200°C, and a reaction time of 1 hour, yielded the lowest lithium extraction rates, with values ranging from 5.93% to 6.25%. This indicates that a lower temperature and shorter reaction time, combined with a higher ore concentration relative to acid, result in suboptimal lithium recovery.

Test 3, performed at an ore-to-acid ratio of 1:1, a digestion temperature of 300°C, and a reaction time of 2 hours, resulted in intermediate lithium yields, ranging from 8.37% to 10.01%. This suggests that while higher temperatures can enhance extraction, the ore-to-acid ratio and reaction time remain critical factors.

Test 4, conducted at an ore-to-acid ratio of 3:4, a digestion temperature of 175°C, and a reaction time of 3 hours, also resulted in intermediate yields, ranging from 6.72% to 7.46%. This further supports the observation that lower temperatures negatively impact lithium extraction.

The data presented in Table 5 underscores the significant influence of ore-to-acid ratio, digestion temperature, and reaction time on lithium yield. Optimal extraction conditions, as demonstrated by Test 1, involve a higher acid concentration, moderate temperature, and extended reaction time. The variability observed across the different samples suggests potential differences in mineralogical composition or ore reactivity, necessitating further characterization for process optimization.

The data presented in Table 5 reveals suboptimal lithium extraction yields. This observation may be attributed to the mineralogical phase of the ore under investigation. As documented by Ellestad and Milne (1950), α -spodumene exhibits limited solubility in sulfuric acid compared to β -spodumene (Ellestad & Milne, 1950). Consequently, to enhance lithium solubilization, a phase transformation of the spodumene, specifically decrepitation, is deemed necessary.

3.5 Effect of calcination

The selection of calcination temperatures for this series of tests was determined by the temperature range under investigation.

Thermal treatment induces a structural transformation in spodumene, specifically from the α -phase, characterized by a monoclinic crystal structure, to the β -phase, exhibiting a tetragonal crystal structure. This β -spodumene phase is characterized by a lower density ($d=2.4$), increased friability, and enhanced reactivity (Braga *et al.*, 2019). This structural transition occurs at elevated temperatures, facilitating ion exchange reactions (Barbosa *et al.*, 2013 ; Kotsupalo *et al.*, 2009 ; Braga *et al.*, 2019).

The degree of α -spodumene to β -spodumene phase transformation is quantified by the mass differential observed at the conclusion of the experiment. This mass differential is calculated using the following expression (Barbosa *et al.*, 2013):

$$\Delta m = \frac{(M - m) * 100}{M}$$

With **M** : initial sample mass

m : final sample mass after calcination

The data resulting from tests conducted within a temperature range of 750°C to 1050°C, maintained for a duration of two hours, is presented in Table 6. This table provides a comprehensive overview of the effects of varying calcination temperatures on the ore samples, facilitating an analysis of the optimal temperature for phase transformation and subsequent lithium extraction.

Table 6 - Calcination results

N° Essai	Temperature (°C)	Initial mass (g)	SPOD A1		SPOD A2		SPOD T1		SPOD T2	
			Final masses (g)	Δm (%)	Final masses (g)	Δm (%)	Final masses (g)	Δm (%)	Final masses (g)	Δm (%)
1	750	500	470.03	5.99	473.12	5.38	472.09	5.58	470.38	5.92
2	800	500	455.09	8.98	458.91	8.22	458.14	8.37	456.01	8.80
3	850	500	441.02	11.80	443.19	11.36	443.04	11.39	442.69	11.46
4	900	500	380.60	23.88	384.43	23.11	481.91	3.62	382.81	23.44
5	950	500	370.08	25.98	371.84	25.63	372.06	25.59	372.01	25.60
6	1000	500	359.99	28.00	361.92	27.62	361.04	27.79	360.92	27.82
7	1050	500	356.01	28.80	357.03	28.59	357.07	28.59	358.05	28.39

Table 6 presents the mass changes observed in spodumene samples SPOD A1, SPOD A2, SPOD T1, and SPOD T2 after calcination at temperatures ranging from 750°C to 1050°C for a duration of two hours. The table provides both the final masses and the percentage mass loss (Δm) for each sample at each temperature.

A trend of increasing mass loss with rising temperature is evident across all samples. At 750°C, the mass loss is relatively low, ranging from 5.38% to 5.99%. As the temperature increases to 800°C, the mass loss rises to approximately 8.22% to 8.98%. This indicates the initiation of structural changes within the spodumene, likely associated with the α - to β -phase transition.

A significant increase in mass loss is observed at 850°C, reaching approximately 11.36% to 11.80%. This suggests that the phase transformation is progressing significantly at this temperature. Further increases in temperature to 900°C result in substantial mass losses, ranging from 23.11% to 23.88% for SPOD A1, A2, and T2, however, for SPOD T1 the mass loss is only 3.62%. This deviation in SPOD T1 may reflect a difference in the mineralogical composition or structural properties of that specific sample.

At 950°C, the mass loss continues to rise, reaching approximately 25.59% to 25.98%. Further increases to 1000°C and 1050°C result in mass losses of approximately 27.62% to 28.80%, indicating that the phase transformation is nearing completion.

The observed mass loss is attributed to the release of volatile components and structural changes within the spodumene during calcination. The data suggests that temperatures above 900°C are particularly effective in inducing significant mass loss, likely associated with the desired α - to β -phase transition. The variation between samples may reflect different starting mineral compositions.

Table 6 demonstrates a direct correlation between increasing calcination temperature and mass loss, indicative of the α - to β -spodumene phase transformation. The observed mass

variations across samples underscore the significant influence of calcination temperature on the resultant product.

The data further reveals a proportional relationship between calcination temperature and the extent of α - to β -spodumene phase transformation; elevated temperatures result in a more pronounced phase transition.

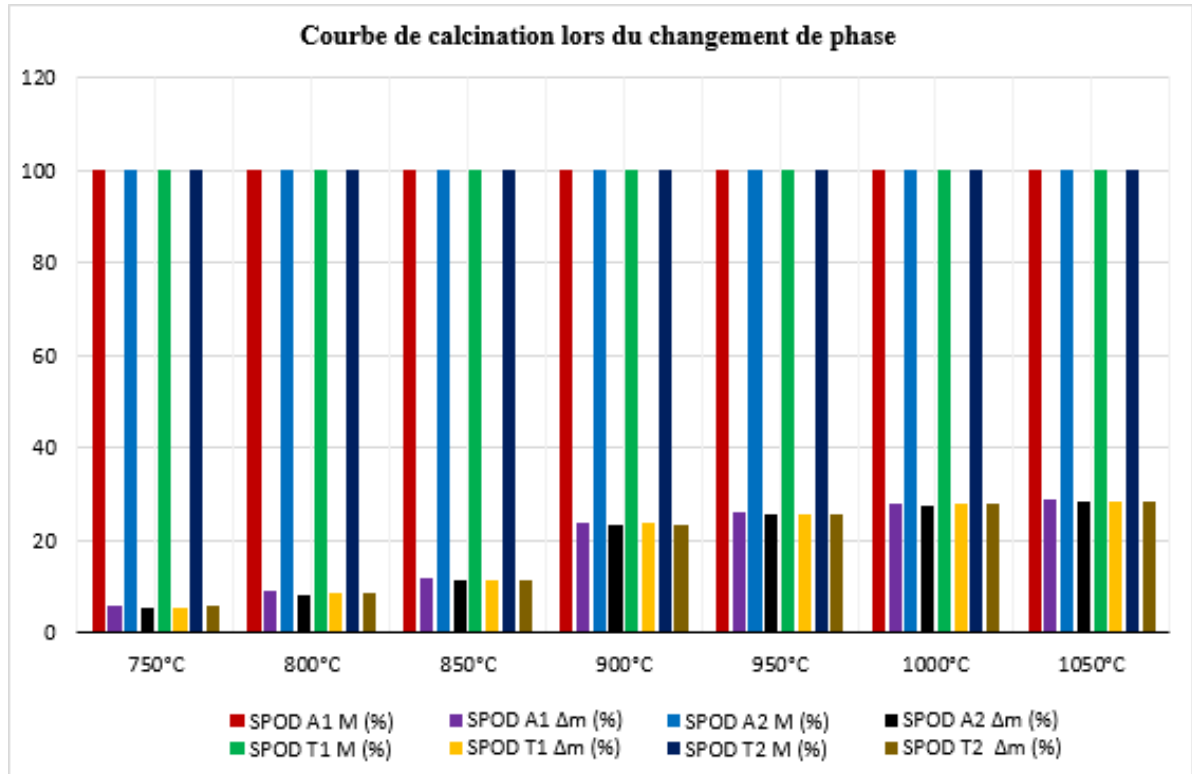


Figure 4. Calcination evolution curve during phase transformation

Mass, a parameter directly correlated with density, serves as an analytical tool for elucidating the phenomena occurring during calcination. As established by Ellestad and Milne (1950), β -spodumene exhibits a significantly lower density compared to α -spodumene (Braga *et al.*, 2019 ; Ellestad & Milne, 1950).

The data reveals a substantial mass differential within the temperature range of 900°C to 1050°C, indicative of the formation of the lower-density β -spodumene phase (approximately 2.4 g/cm³). This phase transformation is visually represented in Figure 4.

3.6 Effect of sulfuric acid digestion

A series of tests was conducted for each calcination temperature range, systematically varying digestion parameters, specifically the ore-to-acid ratio, digestion temperature, and reaction time.

Table 6 - Different factors and levels

Factors		Levels						
		1	2	3	4	5	6	7
A	Calcination temperature (°C)	750	800	900	900	950	1000	1050
B	Ore/acid ratio	3 : 4	3 : 4	3 : 4	3 : 4	3 : 4	3 : 4	3 : 4
C	Digestion temperature (°C)	250	250	250	250	250	250	250
D	Digestion time (minutes)	180	180	180	180	180	180	180

Table 7 presents the experimental design for a series of tests, detailing the varied levels of four critical factors: calcination temperature (A), ore-to-acid ratio (B), digestion temperature (C), and digestion time (D).

The calcination temperature (Factor A) was systematically varied across seven levels, ranging from 750°C to 1050°C, to assess its impact on the spodumene's phase transformation and subsequent lithium extraction. This range was selected based on prior observations indicating a significant phase transition within this temperature window.

The ore-to-acid ratio (Factor B) was maintained at a constant 3:4 across all test levels. This deliberate consistency allows for the isolation and evaluation of the calcination temperature's influence, eliminating potential confounding effects from variations in acid concentration.

The digestion temperature (Factor C) was also held constant at 250°C throughout the experimental series. This fixed parameter ensures that variations in lithium extraction are primarily attributable to the calcination temperature and not to changes in the digestion environment.

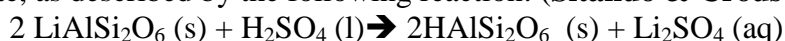
The digestion time (Factor D) was consistently set at 180 minutes (3 hours) across all test levels. This standardized duration provides a uniform reaction period, enabling a direct comparison of lithium extraction yields across the different calcination temperatures.

Table 7 outlines a controlled experimental framework designed to systematically investigate the effect of calcination temperature on lithium extraction, while maintaining consistent ore-to-acid ratio, digestion temperature, and digestion time. This approach allows for a focused analysis of the calcination temperature's impact on the overall process efficiency.

The process leverages the enhanced reactivity of β -spodumene with sulfuric acid. Contact between the acid and the thermally pre-treated material is established at a temperature of 250°C.

An acid excess of at least 30% is required to ensure proton availability following reactions with impurities such as potassium and sodium. Depending on the ore's lithium content, the acid excess may reach 140% (**Dessemond et al., 2019**).

The β -spodumene phase readily reacts with sulfuric acid, yielding soluble lithium sulfate, as described by the following reaction: (**Sitando & Crouse, 2011**)



The effect of digestion is studied in order to improve sulfuric acid diffusion and promote the substitution of H^+ ions by Li^+ . (**Ellestad & Milne, 1950**)

The results obtained after processing are shown in the table below.

Table 7- Optimum spodumene conditions obtained from the experiment

Essay N °	Sample code	Calcination temperature (°C)	M/A	Digestion temperature (°C)	Digestion time (min)	Li yield (%)
1	SPOD A1	750	3/4	250	180	51.25
2	SPOD A2		3/4	250	180	48.93
3	SPOD T1		3/4	250	180	52.61
4	SPOD T2		3/4	250	180	54.01
5	SPOD A1	800	3/4	250	180	54.75
6	SPOD A2		3/4	250	180	52.43
7	SPOD T1		3/4	250	180	56.11
8	SPOD T2		3/4	250	180	57.51
9	SPOD A1		3/4	250	180	59.51
10	SPOD A2		3/4	250	180	57.19

11	SPOD T1	850	3/4	250	180	60.87
12	SPOD T2		3/4	250	180	62.27
13	SPOD A1	900	3/4	250	180	70.01
14	SPOD A2		3/4	250	180	67.69
15	SPOD T1		3/4	250	180	71.37
16	SPOD T2		3/4	250	180	72.77
17	SPOD A1	950	3/4	250	180	83.49
18	SPOD A2		3/4	250	180	81.17
19	SPOD T1		3/4	250	180	84.85
20	SPOD T2		3/4	250	180	86.25
21	SPOD A1	1000	3/4	250	180	91.07
22	SPOD A2		3/4	250	180	89.75
23	SPOD T1		3/4	250	180	92.43
24	SPOD T2		3/4	250	180	93.83
25	SPOD A1	1050	3/4	250	180	95.02
26	SPOD A2		3/4	250	180	93.70
27	SPOD T1		3/4	250	180	96.38
28	SPOD T2		3/4	250	180	96.78

Table 8 presents the lithium extraction yields obtained from spodumene samples SPOD A1, SPOD A2, SPOD T1, and SPOD T2 across varying calcination temperatures, while maintaining a constant ore-to-acid ratio (3/4), digestion temperature (250°C), and digestion time (180 minutes).

The data reveals a clear correlation between calcination temperature and lithium yield. At a calcination temperature of 750°C (Essays 1-4), the lithium yields range from 48.93% to 54.01%. As the calcination temperature increases to 800°C (Essays 5-8), the yields slightly improve, ranging from 52.43% to 57.51%.

A more significant increase in lithium yield is observed at 850°C (Essays 9-12), with yields ranging from 57.19% to 62.27%. At 900°C (Essays 13-16), a further substantial increase is noted, with yields ranging from 67.69% to 72.77%.

The highest lithium yields are achieved at calcination temperatures of 950°C, 1000°C, and 1050°C. At 950°C (Essays 17-20), yields range from 81.17% to 86.25%. At 1000°C (Essays 21-24), yields range from 89.75% to 93.83%. Finally, at 1050°C (Essays 25-28), the highest yields are observed, ranging from 93.70% to 96.78%.

The data presented in Table 8 demonstrates a direct correlation between increasing calcination temperature and lithium extraction yield, under constant ore-to-acid ratio, digestion temperature, and time. This correlation is attributed to the enhanced α - to β -spodumene phase transformation at elevated temperatures, resulting in increased reactivity with sulfuric acid.

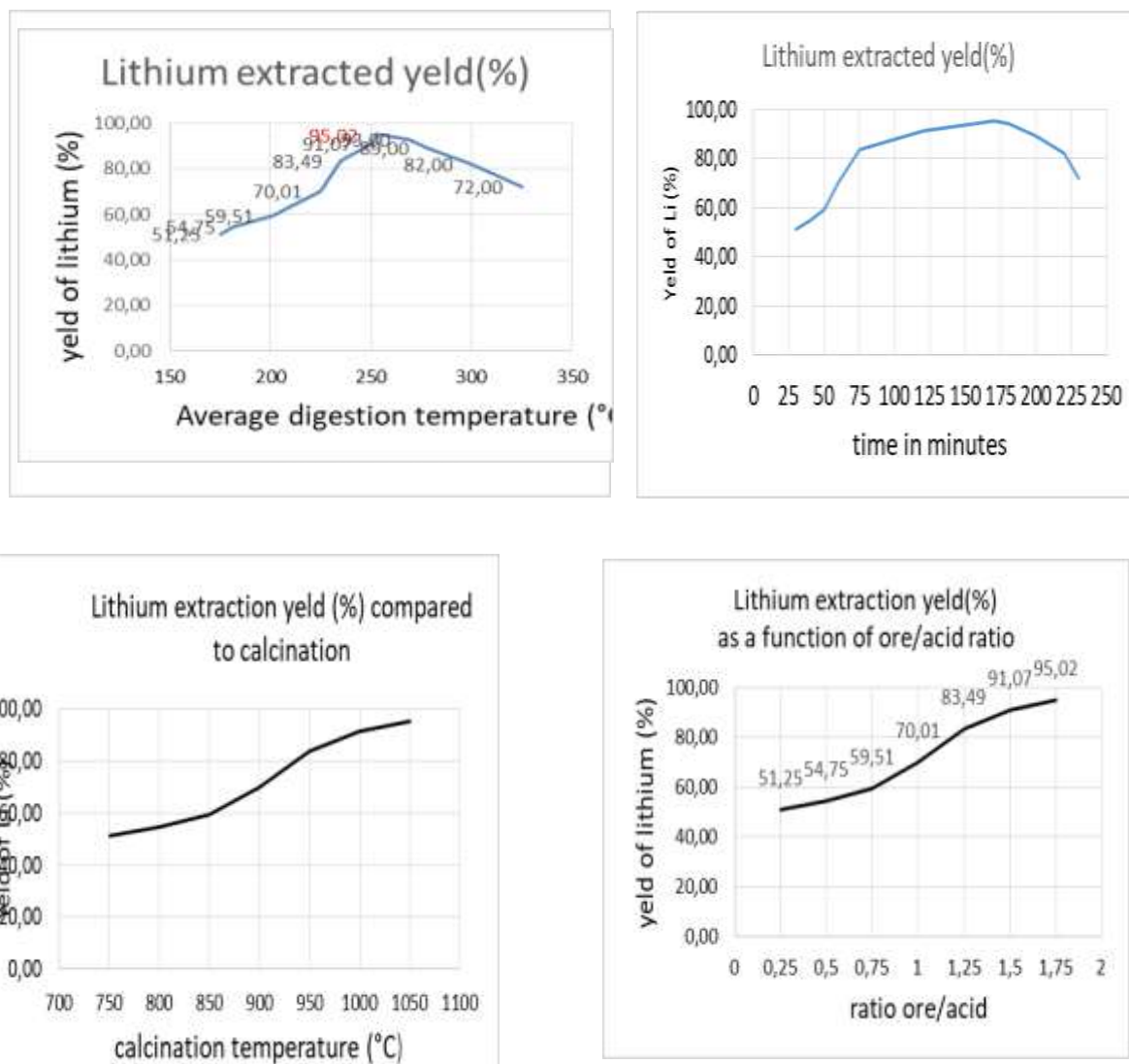


Figure 5. Parametric curves influencing lithium extraction

Optimal lithium solubilization, exceeding 95%, was achieved in tests 25 through 28. These tests utilized an ore calcination temperature of 1050°C, a 3/2 ore-to-acid ratio, a 250°C digestion temperature, and a 3-hour digestion time. Figure 5 visually represents the influence of the controlled factors on lithium extraction yields.

a. Influence of temperature and digestion time

Lithium recovery yield demonstrates a strong dependence on digestion temperature and time. Temperatures exceeding 250°C do not significantly enhance diffusion, as sulfuric acid undergoes partial vaporization (Guo et al., 2017).

Optimal extraction conditions were identified at a digestion temperature of 250°C and a duration of 180 minutes, resulting in a lithium yield of 92.02%. This finding aligns with observations reported by Garrett (2004), who documented comparable results using approximately 50% acid at a digestion temperature of 250°C on spodumene (Lajoie-Leroux et al., 2018 ; Garrett, 2004).

The phenomenon of reduced diffusion at elevated temperatures can be attributed to the volatility of sulfuric acid. As temperature increases, the acid's vapor pressure rises, leading to a decrease in its concentration within the reaction medium. This reduced concentration

diminishes the acid's ability to effectively leach lithium from the spodumene matrix. Furthermore, the kinetics of the solid-liquid reaction between the acid and the mineral may not improve proportionally with temperature beyond a certain point.

The consistency of the observed optimal extraction temperature across independent studies reinforces the robustness of this finding. A digestion temperature of 250°C appears to strike a balance between enhancing reaction kinetics and minimizing acid vaporization, thereby maximizing lithium recovery. The 180-minute duration likely provides sufficient time for the reaction to reach equilibrium, ensuring efficient lithium dissolution. The ore/acid ratio of 3/2 also appears to provide the necessary acid concentration for optimal results.

b. Influence du rapport minéral / acide

Figure 5 indicates that manipulating acid excess results in marginal yield improvements. However, this approach is limited by acid consumption due to reactions with impurities (Lajoie-Leroux *et al.*, 2018; Guo *et al.*, 2017).

Optimal lithium extraction is achieved at a digestion temperature of approximately 250°C, utilizing a slightly elevated ore-to-acid ratio of 3:2. Temperatures exceeding 250°C lead to a substantial decrease in yield, attributed to significant acid volatilization and accompanying gas release.

The observed decline in yield at higher temperatures can be explained by the increased vapor pressure of sulfuric acid. As temperature rises, the acid's volatility increases, resulting in a reduction of its effective concentration in the reaction medium. This decrease in acid concentration diminishes its ability to effectively leach lithium from the spodumene matrix. Furthermore, the evolution of gas, likely sulfur oxides, indicates thermal decomposition of the sulfuric acid, further contributing to acid loss and potential interference with the desired reactions. The 3:2 ratio seems to optimize the acid concentration for the solid liquid reaction, without causing excessive volatilization.

IV. Conclusion

Spodumene and lepidolite constitute pivotal lithium sources, essential for fulfilling escalating global demand. Their inherent abundance and elevated lithium concentrations render them indispensable resources. The diverse applications of mined lithium, spanning battery technology, metallurgy, and pharmacology, underscore its fundamental role across numerous industrial domains.

The potential spodumene and lepidolite deposits in Madagascar present a strategic opportunity, offering significant economic and industrial prospects for the nation. The methodology delineated for lithium carbonate production emphasizes the critical influence of 98% sulfuric acid concentration and a 3-hour firing duration, parameters that yield an enhanced and more precise lithium recovery rate.

This study provides a valuable contribution to the understanding and exploitation of lithium resources, positioning Madagascar as a potential participant in the global lithium supply chain. The results underscore the significance of specific extraction parameters, offering practical guidelines for the optimal utilization of Madagascar's spodumene and lepidolite deposits.

References

- Barbosa, L. I., Valente, G., Orosco, R. P., & Gonzalez, J. A. (2013). Lithium extraction from β -spodumene through chlorination with chlorine gas. *Minerals Engineering*, 50-51, 29–34.
- Braga, P., França, S., Neumann, R., Rodriguez, M., & Rosales, G. (2019). Alkaline process for extracting lithium from Spodumene. *Hydroprocess*, 2–3.
- Deberitz, J.; Boche, G. Lithium und seine Verbindungen-Industrielle, medizinische und wissenschaftliche Bedeutung. *Chem. Unserer Zeit* 2003, 37, 258–266. [CrossRef]
- Dessemond, C., Lajoie-Leroux, F., Soucy, G., Laroche, N., & Magnan, J.-F. (2019). Spodumene: The lithium market, resources and processes. ¹ *Minerals*, 9(12), 765. <https://doi.org/10.3390/min9120765>
- Dinh, T. T. H. (2015). *Processing of Vietnamese lithium ores to produce LiCl* [Doctoral dissertation, Albert-Ludwigs-Universität Freiburg im Breisgau].
- Ellestad, R. B., & Milne, K. L. (1950). *Method of extracting lithium values from spodumene ores*. United States Patent Application 2,109.
- Fosu, A. Y., Kanari, N., Vaughan, J., & Chagnes, A. (2020). Literature review and thermodynamic modelling of roasting processes for lithium extraction from spodumene. *Metals*, 10(10), 1312. <https://doi.org/10.3390/met10101312>
- Garrett, D. E. (2004). Lithium. In **Handbook of lithium and natural calcium chloride. Their deposits, processing, uses and properties** (pp. 1–235). Elsevier Academic Press.
- Garrett, D.E. *Handbook of Lithium and Natural Calcium Chloride*; Elsevier: Amsterdam, The Netherlands, 2004; ISBN 0080472907.
- GB/T51382. 2019. Standard for process design of lithium refinery. China Ministry of Housing and Urban-Rural Development, China State Administration for Market Regulation (in Chinese).
- Gmar, S., & Chagnes, A. (2019). Recent advances on electrodialysis for the recovery of lithium from primary and secondary resources. *Hydrometallurgy*, 189, 105124. <https://doi.org/10.1016/j.hydromet.2019.105124>.
- Guo, H., Kuang, G., Wang, H., Wang, H., & Zhao, X. (2017). Investigation of enhanced leaching of lithium from α -spodumene using hydrofluoric and sulfuric acid. *Minerals*, 7(12), 241. <https://doi.org/10.3390/min7120241>.
- Habashi, F. (1997). Alkali metals. In *Handbook of extractive metallurgy* (pp. 2029–2051). Wiley-VCH.
- Holleman, A. F., Wiberg, E., & Wiberg, N. (2016). *Grundlagen und Hauptgruppenelemente: Band 1: Grundlagen und Hauptgruppenelemente* (103rd ed.). De Gruyter.
- Kondas, J., & Jandová, J. (2006). Lithium extraction from zinnwaldite waste after gravity dressing of Sn-W ores. *Acta Metallurgica Slovaca*, 197–202.
- Kotsupalo, N. P., Isupov, V. P., & Ryabtsev, A. D. (2009). Prospects for the use of lithium-bearing minerals. *Theoretical Foundations of Chemical Engineering*, 43(6), 800–809.
- Kuang, G., Liu, Y., Li, H., Xing, S. Z., Li, F. J., & Guo, H. (2018). Extraction of lithium from β -spodumene using sodium sulfate solution. *Hydrometallurgy*, 177, 49–56. <https://doi.org/10.1016/j.hydromet.2018.02.015>
- Lajoie-Leroux, F., Dessemond, C., Soucy, G., Laroche, N., & Magnan, J.-F. (2018). Impact of the impurities on lithium extraction from β -spodumene in the sulfuric acid process. *Minerals Engineering*, 126, 168–176. <https://doi.org/10.1016/j.mineng.2018.06.009>.
- Marcinov, V., Klimko, J., Takáčová, Z., Pirošková, J., Miškuřová, A., Sommerfeld, M., Dertmann, C., Friedrich, B., & Oráč, D. (2023). Lithium production and recovery

- methods: Overview of lithium losses. *Metals*, 13(7), 1213. <https://doi.org/10.3390/met13071213>
- Margarido, F., Vecceli, N., Durao, F., Guimarães, C., & Nogueira, C. A. (2014). Mineralo-metallurgical processes for lithium recovery from pegmatitic ores. *Comunicações Geológicas*, 795–798.
- Meshram, P., Pandey, B. D., & Mankhand, T. R. (2014). Extraction of lithium from primary and secondary sources by pre-treatment, leaching and separation: A comprehensive review. *Hydrometallurgy*, 150, 192–208. <https://doi.org/10.1016/j.hydromet.2014.10.012>
- Nandihalli, N., Chouhan, R. K., Kuchi, R., & Hlova, I. Z. (2024). Aspects of spodumene lithium extraction techniques. *Sustainability*, 16(19), 8513. <https://doi.org/10.3390/su16198513>
- Nogueira, C. A. (1996). *Extração de lítio de recursos nacionais provas de acesso a assistente de investigação*. LNETI..
- Nogueira, C. A., Margarido, F., Vecceli, N., Durao, F. O., & Guimarães, C. (2014). Comparison of processes for lithium recovery from Lepidolite by H₂SO₄ digestion or HCl leaching. In *Proceedings of the International Conference on Mining, Material and Metallurgical Engineering*.
- Raherisoa, H. (2017). *Caractérisation de la tourmaline et des minéraux associés de la vallée de Sahatany, corrélation géologie – géologie – gemmologie* [Thèse de doctorat].
- Rakotoarisoa, N. D. (2003). *Contribution à l'étude monographique des gites pegmatitiques de région de Betafo-Antsirabe. Interprétation structurale d'images Landsat* [Mémoire de DEA]..
- Rakotovao, S. R. (2004). *Contribution à l'étude des pegmatites Rhondizites de la région d'Ibity (Gisement de Manjaka et d'Antandrokomby)* [Mémoire de DEA, Université d'Antananarivo].
- Ran, J. W., Liu, X., Pei, J., & Yin, W. X. (2016). Development of production technology of lithium resource in China. *Guangzhou Chemical Industry*, 44(13), 4–6. <https://doi.org/10.3969/j.issn.1001-9677.2016.13.002>
- Ranoroso, N. J. (1986). *Étude minéralogique et micromonométrique des pegmatites du champ de la Sahatany* [Thèse de doctorat, Université Paul Sabatier].
- Sahoo, S. K., Tripathy, S. K., Nayak, A., Hembrom, K. C., Dey, S., & Rath, R. K. (2024). Beneficiation of lithium bearing pegmatite rock: A review. *Mineral Processing and Extractive Metallurgy Review*, 45(1), 1–27. <https://doi.org/10.1080/08827508.2022.2117172>
- Schmidt, M. (2017). *Rohstoffrisikobewertung Lithium*. Bundesanstalt für Geowissenschaften und Rohstoffe (BGR), Deutsche Rohstoffagentur.
- Sitando, O., & Crouse, P. (2011). Processing Zimbabwean petalite to obtain lithium carbonate. *International Journal of Mineral Processing*, 98(1-2), 45–50.
- Su, H., Zhu, Z. W., Wang, L. N., & Qi, T. (2019). Research progress in extraction and recovery of lithium from hard-rock ores. *CIESC Journal*, 70(1), 10–23. <https://doi.org/10.11949/j.issn.0438-1157.20180465>.
- Swain, B. (2017). Recovery and recycling of lithium: A review. Separation and Purification Technology, 172, 388–403. <https://doi.org/10.1016/j.seppur.2016.08.031>
- Tadesse, B., Makuei, F., Albijanic, B., & Dyer, L. (2019). The beneficiation of lithium minerals from hard rock ores: A review. *Minerals Engineering*, 131, 170–184. <https://doi.org/10.1016/j.mineng.2018.11.023>
- Tan, B., Liu, X. H., Liu, X. D., & Yi, M. G. (2021). Study on law of lithium extraction and impurity removal from spodumene leaching solution. *Inorganic Chemicals Industry*, 53(4), 56–60. <https://doi.org/10.11962/1006-4990.2020-0315>

- U.S. Geological Survey. (2023). *Mineral commodity summaries 2023*. U.S. Geological Survey.
- Zhu, Z. H., Zhu, C. L., Wen, X. M., Zhuge, Q., & Ling, B. P. (2008). Progress in production process of lithium carbonate. *Journal of Salt Lake Research*, 16(3), 64–72.